CrossMark

RESEARCH ARTICLE

Photochemical defluorination of aqueous perfluorooctanoic acid (PFOA) by Fe^0/GAC micro-electrolysis and VUV-Fenton photolysis

Li-hong Zhang[1] · Jian-hua Cheng[1,2] · Xia You[1] · Xiao-yan Liang[1] · Yong-you Hu[1,2]

Abstract Perfluorooctanoic acid (PFOA) is extremely persistent and bioaccumulative in the environment; thus, it is very urgent to investigate an effective and moderate technology to treat the pollution of PFOA. In this study, a process combined iron and granular activated carbon (Fe^0/GAC) micro-electrolysis with VUV-Fenton system is employed for the remediation of PFOA. Approximately 50 % PFOA ($10\ mg\ L^{-1}$) could be efficiently defluorinated under the following conditions: pH 3.0, dosage of Fe $7.5\ g\ L^{-1}$, dosage of GAC $12.5\ g\ L^{-1}$, and concentration of H_2O_2 $22.8\ mmol\ L^{-1}$. Meanwhile, during the process, evident defluorination was observed and the concentration of fluoride ion was eventually $3.23\ mg\ L^{-1}$. The intermediates including five shorter-chain perfluorinated carboxylic acids (PFCAs), i.e., C7, C6, C5, C4, and C3, were also analyzed by high-performance liquid chromatography tandem mass spectrometry (HPLC/MS/MS) and defluorination mechanisms of PFOA was proposed, which involved photochemical of OH·, direct photolysis (185-nm VUV), and photocatalytic degradation of PFOA in the presence of Fe^{3+} (254-nm UV).

✉ Jian-hua Cheng
jhcheng@scut.edu.cn

1 Ministry of Education Key Laboratory of Pollution Control and Ecological Remediation for Industrial Agglomeration Area, College of Environment and Energy, South China University of Technology, Guangzhou 510006, China
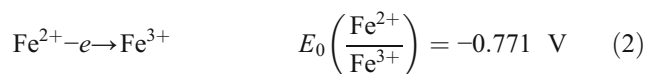
2 Hunan Key Laboratory of Applied Environmental Photocatalysis, Changsha University, Changsha 410022, People's Republic of China

Introduction

Perfluorooctanoic acid (PFOA) has been extensively used in numerous industrial and commercial trades, including chemical industry, textile industry, coating, and paper manufacturing industry (Poothong et al. 2012)—due to its specific characteristics such as high surface activity, high chemical stability, and thermal and acid resistance (Houde et al. 2006). Recently, it has been detected in various environmental media (Dinglasan-Panlilio et al. 2014; Heydebreck et al. 2015; Shoeib et al. 2006), wildlife (Yen Le and Peijnenburg 2013; Wania 2007; Dai et al. 2006), and humans (Yeung et al. 2013; Geiger et al. 2014; Lau et al. 2007). The bioaccumulation of PFOA has been revealed (Gisey and Kannan 2001), and its toxicological properties, including liver toxicity, neural toxicity (Hu et al. 2012; Johansson et al. 2009), embryonic developmental toxicity (Ding et al. 2013), endocrine disruption (Abbott et al. 2012), and potential carcinogenicity (Florentin et al. 2011; Butenhoff et al. 2012), have also been detected. Considering the unique properties of PFOA, especially the strong carbon-fluorine bond (C–F; $116\ kcal\ mol^{-1}$) (Blake et al. 1997) and the high oxidation potential ($E_0 = 3.6\ V$), PFOA is highly stable under chemical and thermal destructions. Therefore, the traditional wastewater treatment methods, such as biodegradation and chemical degradation, were useless to decompose PFOA. Moreover, a majority of advanced oxidation technologies were also unable to eliminate PFOA effectively. According to previous reports (Lee et al. 2010; Yang et al. 2013), PFOA could be effectively decomposed by sulfuric acid radical oxidation and sonochemical degradation. However, the decomposition required strict reaction

conditions and high energy consumption. Moreover, PFOA could be degraded by photocatalysis and photochemistry oxidation under mild reaction conditions, which were seem to be slow and inefficient. Therefore, the investigation of PFOA elimination under mild conditions has become an attractive target in the field of environmental science.
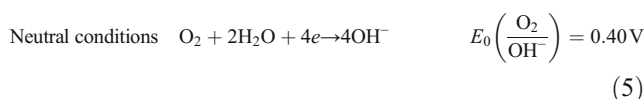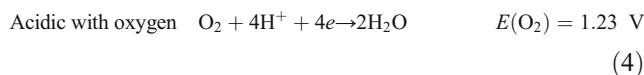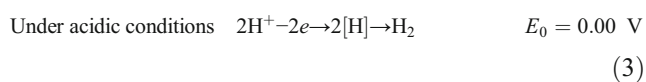
It has been already demonstrated that PFOA could be decomposed efficiently by VUV radiation (<200 nm), as PFOA had strong absorption in 185-nm VUV light region (Vaalgamaa et al. 2011). However, the major wavelengths emitted from commercial VUV lamps are longer than 200 nm, and the 185 nm VUV light was only 12–15 % of the entire spectral range. Thus, the direct photolysis of PFOA only consumed a small part of photon energy from VUV light. On the other hand, it was reported that ferric ions could form coordination compound with PFOA, and the electron transferred from compound to metal under the 254-nm UV light radiation, resulting in the degradation of PFOA. Cheng et al. (2014) reported that PFOA could be eliminated by VUV/Fe^{3+} system, and the defluorination rate constant of PFOA in the presence of 20 μM ferric ion was approximately 2.6 times higher than that observed in VUV treatment alone.

In recent years, iron and granular activated carbon (Fe^0/GAC) micro-electrolysis has been widely applied in wastewater treatment, including dyes (Huang et al. 2013a), landfill leachate (Ying et al. 2012), petroleum wastewaters (Li et al. 2010; Guan et al. 2012), and coking wastewater (Liu et al. 2012; Lv et al. 2011). The researchers have already paid attention to the combination of Fe^0/GAC micro-electrolysis with other technologies, such as Fenton process (Wang et al. 2013), anaerobic treatment (Huang et al. 2013b), and ultrasound pyrolysis (Zhou et al. 2013). A large number of proto batteries will be formed, when iron and GAC were in touched with electrolyte solution (Huang et al. 2013b; Fan et al. 2009; Zhu et al. 2014). Iron as anode lost two electrons to form ferrous ion. The GAC as cathode accelerated the reduction or oxygen of the pollutants by accepting electrons and transferring the electrons. The reactions could be expressed as follows (Zhang et al. 2015; Qin et al. 2012):

Anodic oxidation

$$Fe-2e\rightarrow Fe^{2+} \qquad E_0\left(\frac{Fe^{2+}}{Fe}\right) = -0.44 \text{ V} \qquad (1)$$

$$Fe^{2+}-e\rightarrow Fe^{3+} \qquad E_0\left(\frac{Fe^{2+}}{Fe^{3+}}\right) = -0.771 \text{ V} \qquad (2)$$

Cathodic reduction

$$\text{Under acidic conditions} \quad 2H^+-2e\rightarrow 2[H]\rightarrow H_2 \qquad E_0 = 0.00 \text{ V} \qquad (3)$$

$$\text{Acidic with oxygen} \quad O_2 + 4H^+ + 4e\rightarrow 2H_2O \qquad E(O_2) = 1.23 \text{ V} \qquad (4)$$

$$\text{Neutral conditions} \quad O_2 + 2H_2O + 4e\rightarrow 4OH^- \qquad E_0\left(\frac{O_2}{OH^-}\right) = 0.40\,\text{V} \qquad (5)$$
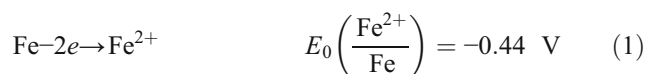
Fe^{2+} and the new eco-hydrogen [H] had high chemical activity, which could break organic matter chain and change the organic functional groups. In the presence of H_2O_2, Fe^{2+} and H_2O_2 could react and generate Fe^{3+} and OH· radicals. As known, the complex which generated between Fe^{3+} and PFOA was conducive to the decomposition of PFOA under 254-nm UV light radiation. Therefore, the introduction of Fe^0/GAC micro-electrolysis in VUV system could greatly improve the utilization of light intensity and the defluorination of PFOA. Researchers (Tang et al. 2012) also conducted that OH· radicals could effectively degrade perfluorinated carboxylic acids (PFCAs) by weakening the C-F bond with the aid of other substrate or introducing external high energies such as UV radiation. Hence, we anticipate that PFOA might be mineralized by OH· radicals under VUV irradiation. Furthermore, whether Fe^0/GAC micro-electrolysis could improve the elimination of PFOA was still unknown.

The main objectives of this study were to investigate the efficiency and mechanism of photochemical defluorination of PFOA in the combined Fe^0/GAC micro-electrolysis with VUV-Fenton system. Firstly, the effects of various factors on the photochemical defluorination of PFOA were discussed. Secondly, the intermediate products were determined using HPLC/MS/MS. Eventually, the potential defluorination mechanism and degradation pathways of PFOA were proposed.

Materials and method

Chemical reagents

Perfluorooctanoic acid ($C_7F_{15}COOH$, PFOA, 95 %) and perfluoroheptanoic acid ($C_6F_{13}COOH$, PFHpA, 98 %) were purchased from Alfa Company, USA. Perfluorohexanoic acid ($C_5F_{11}COOH$, PFHxA, 98 %) and perfluoropentanoic acid (C_4F_9COOH, PFPeA, 98 %) were obtained from Tokyo Kasei, Japan. Perfluorobutanoic acid (C_3F_7COOH, PFBA, 99 %) and trifluoroacetic acid (CF_3COOH, TFA, 97 %) were purchased from Adamas Reagent, Switzerland. Perfluoroacyl acid (C_2F_5COOH, PFPA, 97 %) was bought from Acros Organics, Belgium. Ferrous sulfate heptahydrate ($FeSO_4\cdot 7H_2O$), hydrogen peroxide (H_2O_2, 30 %), ammonium acetate (CH_3COONH_4), glacial acetic acid (CH_3COOH), sodium fluoride (NaF), sodium acetate ($C_2H_9NaO_5$), hydroxylamine hydrochloride ($NH_2OH\cdot HCl$), phenanthroline ($C_{12}H_8N_2\cdot H_2O$), sulfuric acid (H_2SO_4), chloride (HCl), and sodium

hydroxide (NaOH) were purchased from Guangzhou Chemical Reagent Factory (Guangzhou, China). Ammonium ferrous sulfate ($NH_4Fe(SO_4) \cdot 7H_2O$), iron powder, and commercial GAC were obtained from Tianjin Fuchen Chemical Reagents Factory (Tianjin, China). Trisodium citrate dehydrate ($C_6H_5Na_3O_7 \cdot 7H_2O$) was purchased from Sinopharm Chemical Reagent Co., Ltd (China). All other reagents were of analytical grade from Beijing Chemical Factory (Beijing, China). And, ultrapure water supplied by the Millipore Milli-Q ultrapure water system (USA) with a conductivity of 18.2 mΩ cm at 25 °C was used in all experiments. All chemicals were used as received without any further purification.

Preparation of GAC

GAC was immersed in PFOA solution of 10 mg L^{-1} for 24 h to achieve the adsorbing-desorbing equilibrium and then washed with ultrapure water in order to eliminate the interference of the impurities and the adsorption of PFOA. Finally, the treated GAC was put in a vacuum drying chamber for 4 h at 70 °C and sealed for use.

Reaction procedures

Fe^0/GAC micro-electrolysis system was sated before VUV-Fenton system to initially degraded PFOA. The reaction was conducted in a Teflon cylindrical reactor with an inner diameter of 90 mm (Fig. 1a). A stirring paddle was placed in the center of the reactor. Aqueous solution of PFOA was prepared before the experiment and used immediately. The GAC and Fe^0 were stirred well before reaction at a specific mass rate. In a typical run, the mixture was mixed with 10 mg/L PFOA in the reactor. The solution was stirring with the speed of 200 r min^{-1} for 1 h and then proceeded to the VUV-Fenton

system. The initial pH was adjusted to 3.0 by NaOH and HCl except for "solution pH effect" reaction.

The photodegradation reaction was conducted in a Teflon cylindrical reactor with an inner diameter of 75 mm (Fig. 1b). A low-pressure mercury lamp (5 W, Philips Lighting Co., Guangdong, China) emitting mainly 254-nm UV light and a small amount of 185-nm VUV light (12–15 %) was placed at the center of the reactor with quartz tube protection (external diameter 25 mm). In a typical run, the reaction solution after Fe^0/GAC micro-electrolysis treatment was introduced into the reactor. The initial pH was adjusted to 3.0 by NaOH and HCl except for solution pH effect reaction. Then, certain amount of H_2O_2 was added into the reactor. No additional gas was supplied during the entire reaction. The whole photochemical reactions were marched at room temperature for all of the runs. The reaction solutions were sampled for analysis at regular time intervals of 60 min.

Analytical procedures

The concentrations of PFOA and the intermediate products were detected by high-performance liquid chromatography tandem mass spectrometry (HPLC/MS/MS; RRLC/6410B Triple Quard MS, USA). HPLC was used for the separation of PFOA and the intermediates. The multiple reaction monitoring mode (MRM) was used to quantify analysis of PFOA and other shorter-chain PFCAs. HPLC/MS/MS analysis was performed in three separate HPLC/MS/MS runs (methods 1–3) in the MRM mode. Method 1 conducted the PFOA and intermediates in the negative ionization mode, method 2 the compounds in the positive ionization mode, and method 3 the alkylphenolic compounds. Other details could be found in the literatures (Yang et al. 2013; Loos et al. 2008; Loos et al. 2009). Finally, the external standard method was applied to quantify concentrations of PFOA and the intermediate products.
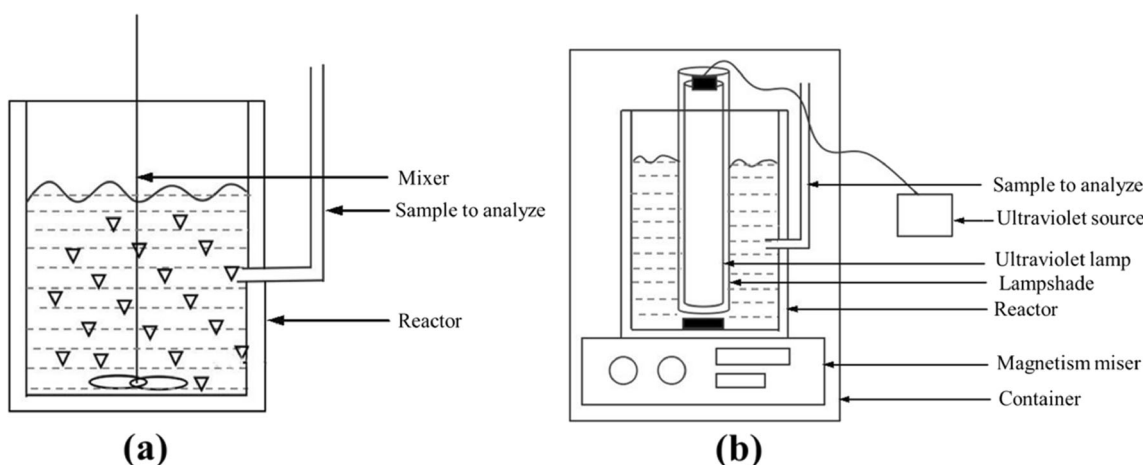

Fig. 1 Schematic representation of reactor **a** iron carbon micro-electrolysis and **b** VUV-Fenton

The concentration of fluoride ion (F^-) in aqueous solution was determined using a fluoride ion selective electrode (PF-1-01, Rex Electric Chemical, Shanghai Instrument Scientific Instrument Co., Ltd) integrated with calomel reference electrode (232, Rex Electric Chemical, Shanghai Instrument Scientific Instrument Co., Ltd). The limit of detection of this means was 0.01 mg L^{-1}. Defluorination ratio of PFOA was calculated as follows:

$$\text{Defluorination ratio} = \frac{C_{F^-} \times 414}{15 \times C_0} \times 100 \ \% \qquad (6)$$

where C_{F^-} is concentration of fluoride ion, mM, and C_0 is initial concentration of PFOA, mg L^{-1}. The factor of 15 amounts to the number of fluorine atoms contained in a PFOA molecule. The regression coefficient (R^2) of the calibration curves was 0.9992.

The concentrations of total organic carbon (TOC) were detected by total organic carbon analyzer.

The concentrations of total iron and ferrous were measured using 1,10-phenanthroline spectrophotometric method ($\lambda_{max} - 510$ nm) (Amonette and Templeton 1998); the concentration of Fe^{3+} was calculated as the Fe^{2+} ion concentration subtracted from the total iron concentration.

Results and discussion

Effects of VUV photolysis system on photodegradation of PFOA

The decomposition of PFOA was investigated in the systems of alone VUV and Fe^0/GAC micro-electrolysis coupled with VUV-Fenton. It was well assured that PFOA could be directly decomposed by the deep UV region (<200 nm) light irradiation (Wang et al. 2010; Cao et al. 2010). The experiments showed that the concentration of fluoride ion in solution synchronously increased with the degradation of PFOA (Fig. 2a). The PFOA with initial concentration 10 mg L^{-1} was defluorinated by 185-nm VUV light irradiation, and defluorination ratio attained about 20 % within 2 h (Fig. 2a), which was in good agreement with the results reported by Chen et al. (2007). In addition, defluorination efficiency of PFOA increased to 39 % after 6 h. However, compared to direct photolysis, Fe^0/GAC micro-electrolysis and VUV-Fenton system improved PFOA decomposition. The defluorination ratio of PFOA with an initial concentration of 10 mg L^{-1} approximately reached 47 % for 6-h reaction (Fig. 2a). Moreover, it was found that PFOA could be decomposed by Fe^0/GAC micro-electrolysis through detecting the intermediates of PFOA (Fig. 8a). Lai et al. (2013) found that the macroscopic galvanic cells of the Fe^0/GAC micro-electrolysis system played a key role in degradation of

3,3′-iminobis-propanenitrile. Fe^0/GAC micro-electrolysis was an electrochemical corrosion process occurring between the Fe^0 and GAC in the wastewater, which could generate [H] and O· from electrode action to reduce or oxidize organic pollutants. In addition, Fe^{3+} and OH· were formed between H_2O_2 and Fe^{2+} from Fe^0/GAC micro-electrolysis. It was reported (Tang et al. 2012) that OH^- and UV could break down PFOA. Moreover, it was also reported (Wang et al. 2008) that PFOA could be degraded by UV/Fe^{3+} (254 nm) system. Tang et al. (2012) investigated the removal of PFOA in UV-Fenton systems, and they found that the decomposition of PFOA could be divided into two stage; at the first stage, the defluoriantion and degradation of PFOA was attributed to the generation of OH radicals, and at the second stage, the mineralization of PFOA was mainly due to the complex between PFOA and Fe^{3+} ions. Thus, Fe^0/GAC micro-electrolysis and VUV-Fenton system were worthy of further study according to our results and others' reports.

In order to study the mineralization of PFOA by Fe^0/GAC micro-electrolysis and VUV-Fenton system, the TOC was measured in Fig. 2b. The experiment was selected 50 mg L^{-1} of initial PFOA concentration (the actual value of TOC was 11.59 mg L^{-1}) for improving the accuracy of the TOC determination. As shown in Fig. 2b, TOC gradually reduced with running reaction. That is, TOC was transformed into inorganic carbon (IC). Furthermore, F^- was detected in Fe^0/GAC micro-electrolysis and VUV-Fenton system. This indicated that PFOA was finally mineralized into IC and F^-. The degradation mechanisms of PFOA were particularly discussed in the "Defluorination and decomposition mechanisms of PFOA" section.

Influence of GAC dosage on the defluoridation effect

The effects of GAC dosage (varying from 7.5 to 17.5 g L^{-1}) on defluorination were conducted with 10 mg L^{-1} of initial PFOA concentration and 5 g L^{-1} of Fe dosage, and the results were illustrated in Fig. 3a.

In Fig. 3a, the defluorination efficiency of PFOA at 7 h was 27.8 % at the GAC dosage of 7.5 g L^{-1} and increased dosage of GAC (<12.5 g L^{-1}); defluorination ratio of PFOA quickly improved. However, the defluorination ratio of PFOA decreased gradually once the dosage of GAC was more than 12.5 g L^{-1}. Fe^0 as an anodic metal provided electrons for the pollutant; GAC particles as cathodes were used to form macroscopic galvanic cells contacting with Fe^0 in the Fe^0/GAC micro-electrolysis system. Therefore, the dosage of GAC more or less could all effect on the balance of the primary cell between Fe^0 and GAC and further effected the decomposition of PFOA. Thus, the dosage of GAC 12.5 g L^{-1} was selected in the following researches.
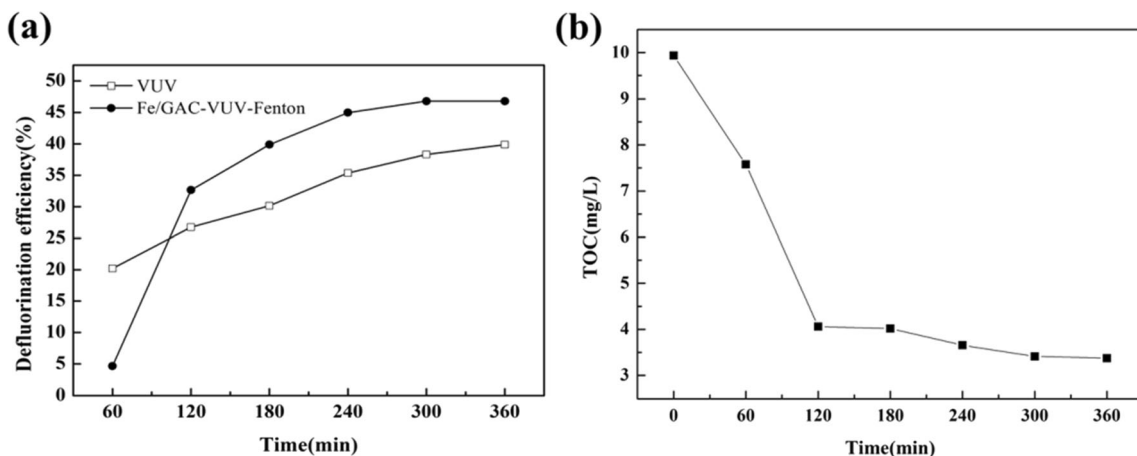
Fig. 2 **a** Photochemical defluorination ratio under VUV and Fe^0/GAC micro-electrolysis and VUV-Fenton systems, $C_{0(PFOA)} = 10$ mg L^{-1}, $pH_0 = 3.0$, $C_{0(Fe)} = 7.5$ g L^{-1}, $C_{0(GAC)} = 12.5$ g L^{-1}, and $[H_2O_2]_0 = 22.8$ mmol L^{-1}. **b** The change of TOC under Fe^0/GAC micro-electrolysis and VUV-Fenton system, $C_{0(PFOA)} = 50$ mg L^{-1}, $pH_0 = 3.0$, $C_{0(Fe)} = 7.5$ g L^{-1}, $C_{0(GAC)} = 12.5$ g L^{-1}, and $[H_2O_2]_0 = 22.8$ mmol L^{-1}

Influence of Fe^0 dosage on the defluoridation of PFOA

In order to study the influence of the Fe^0 dosage on the degradation of PFOA by Fe^0/GAC micro-electrolysis and VUV-Fenton system, the various Fe^0 dosages were analyzed in Fig. 3b. Under the certain amount (<7.5 g L^{-1}), the photochemical reactivity was enhanced with increasing the initial Fe^0 dosage. After 1-h reaction, the defluorination ratio of PFOA reached 3.2 % in the presence of 2.5 g L^{-1} Fe dosage. The defluorination efficiency of PFOA increased to 4.6 % when the Fe^0 concentration was increased to 7.5 g L^{-1}. However, the defluorination ratio of PFOA decreased when the dosage of Fe^0 exceeded 7.5 g L^{-1}, indicating that superfluous Fe^0 might inhibit defluorination of PFOA.

Furthermore, with the change of Fe^0 dosage, the photocatalytic degradation efficiency of PFOA was various (Fig. 3b).

In this section, the photocatalytic decomposition and defluorination of PFOA were attributed to the generation of complex between PFOA and ferric ion under 254-nm UV light radiation, as well as the generation of OH· radicals. Figure 3b shows that removal ratio of PFOA was accelerated with increasing dosage of Fe^0 (<7.5 g L^{-1}). After 7-h reaction, the defluorination efficiency of PFOA was 19.3 % in the presence 2.5 g L^{-1} dosage of Fe^0. Moreover, it greatly enhanced to 43.2 % when the dosage of Fe^0 increased to 7.5 g L^{-1}. However, defluorination ratio of PFOA was decreased when the dosage of Fe^0 further increased to over 7.5 g L^{-1}. Tang et al. (2012) suggested that the decomposition and defluorination efficiencies of PFOA in UV-Fenton systems were 95 and 53.2 % at reaction time of 5 h, respectively. The generation of OH· radicals and the complex between PFOA and Fe^{3+} also were found in Tang's study. Cheng et
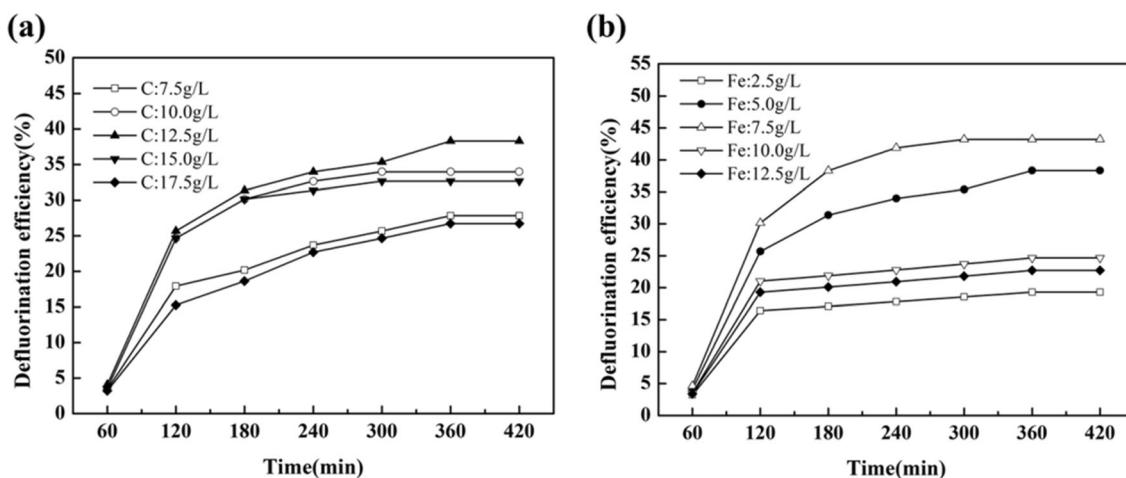

Fig. 3 **a** Effects of GAC dosage on the defluorination of PFOA. **b** Effects of Fe dosage on the defluorination of PFOA. $C_{0(PFOA)} = 10$ mg L^{-1}, $pH_0 = 3.0$, and $[H_2O_2]_0 = 11.4$ mmol L^{-1}

al. (2014) reported that the photochemical reactivity improved when the initial amount of ferric ion increased in the Fe^{3+} concentration range of 20–30 μM by VUV/Fe^{3+} system. Therefore, it was inferred that OH· and the Fe^{3+} ions made a major contribution to the defluorination of PFOA. This will be further discussed below.

Influence of initial pH values on the defluoridation of PFOA

In this section, the effects of initial pH with Fe^0/GAC micro-electrolysis system and VUV-Fenton system on defluorination of PFOA were discussed, respectively.

In Fe^0/GAC micro-electrolysis system, the initial pH value of the wastewater directly affected the potential difference of electrolysis reaction, because the ferric species would precipitate as ferric hydroxides at alkali condition, which made it more difficult to establish a good redox system between H_2O_2 and Fe^{2+}/Fe^{3+}. The various pH value had different influences on the defluorination ratio of PFOA. As shown in Fig. 4a, with an increase of pH (<3.0), the defluorination efficiency improved quickly. It was found that the defluorination ratio of PFOA increased from 27.8 to 43.2 % when pH increased from 2.5 to 3.0 after 7-h reaction (Fig. 4a). However, the defluorination efficiency of PFOA decreased when the initial pH further elevated. Fe^{2+} was produced in Fe^0/GAC micro-electrolysis process and quickly oxidized to Fe^{3+}, which resulted in the solution turned into a deep yellow in air. This could hinder photodegradation reaction in VUV-Fenton. Ferric could generate hydroxide precipitation when the pH of the aqueous solution was more than 4.0, resulting in a negative influence on both Fe^0/GAC micro-electrolysis and VUV-Fenton system. Therefore, pH of 3.0 was chosen in iron carbon micro-electrolysis system.

In VUV-Fenton system, the initial pH of the aqueous solution mainly affected photochemical reactivity. Thus, to study the effects of initial pH on the degradation of PFOA in VUV-Fenton system, five samples with initial pH of 2.5, 3.0, 3.5, 4.0, and 4.5 were investigated (Fig. 4b). As shown in Fig. 4b, the defluorination ratio of PFOA approximately reached 43.21 % at initial pH 3.0 for 7-h reaction. However, a higher or lower pH had an adverse influence on the defluorination efficiency of PFOA. In acidic conditions, PFOA mainly existed in its molecular state ($C_7F_{15}COOH$), while it emerged in its ionic status ($C_7F_{15}COO^-$) in neutral and alkaline conditions. Although PFOA and its intermediate products with ionic status were beneficial to removal under 185-nm VUV light radiation, the system involved in the photocatalytic degradation in the presence of Fe^{3+}, which Fe^{3+} and the free radicals were the vital to the VUV-Fenton system. Moreover, the pH also had an influence on forming of the complex between Fe^{3+} and PFOA. When the pH is more than 4.0, Fe^{3+} could form iron hydroxide precipitation, resulting in the form of complex ($[PFOA-Fe]^{2+}$) that was held back, and the direct photolysis of PFOA also was affected. It was reported (Cheng et al. 2014) that PFOA could exist in the protonated form in the case of lower pH (>2.8), which was not beneficial to the formation of complex between ferric ion and PFOA and electronic transferred. Therefore, acidic condition (pH = 3.0) was conductive to defluorination of PFOA.

Influence of H_2O_2 concentration on the defluoridation of PFOA

The effects of initial H_2O_2 concentrations (0~57 mmol L^{-1}) on the PFOA defluorination ratio were given in Fig. 5. The defluorination efficiency of PFOA reached 21.02 % in the absence of H_2O_2 by Fe^0/GAC micro-electrolysis and VUV-
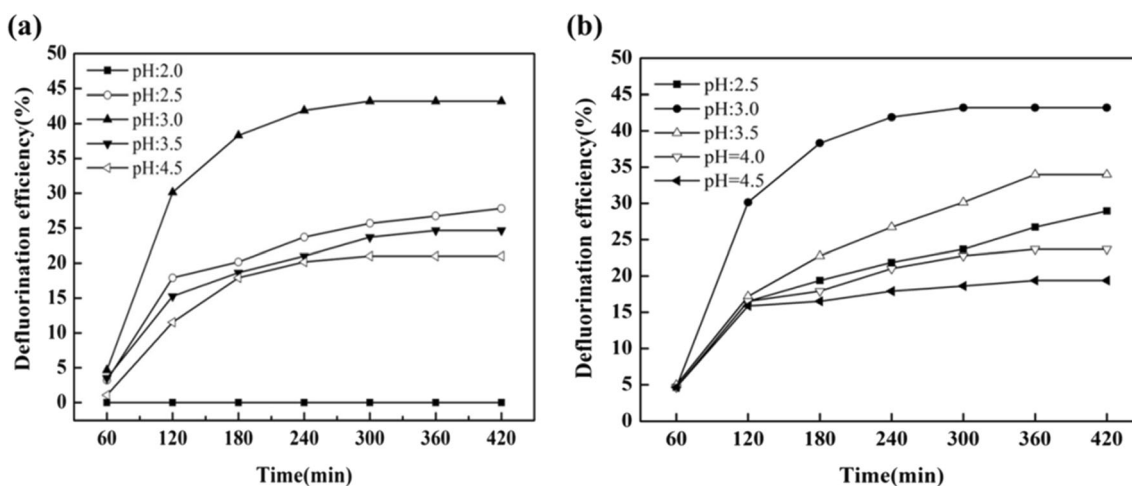

Fig. 4 Effects of pH on the defluorination of PFOA in **a** Fe^0/GAC micro-electrolysis and **b** VUV-Fenton process, $C_{0(PFOA)}$ = 10 mg L^{-1}, $C_{0(Fe)}$ = 7.5 g L^{-1}, $C_{0(GAC)}$ = 12.5 g L^{-1}, and $[H_2O_2]_0$ = 11.4 mmol L^{-1}
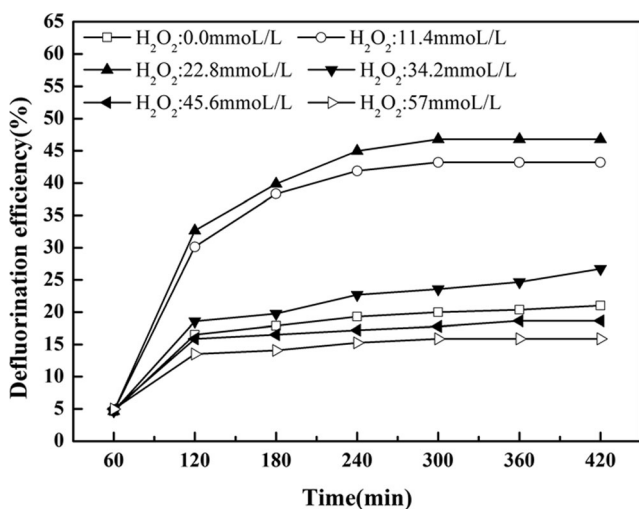
Fig. 5 Effects of H_2O_2 dosage on the defluorination of PFOA, $C_{0(PFOA)} = 10$ mg L^{-1}, $pH_0 = 3.0$, $C_{0(Fe)} = 7.5$ g L^{-1}, and $C_{0(GAC)} = 12.5$ g L^{-1}

Fig. 6 Valence state and content of iron in the system, $C_{0(PFOA)} = 10$ mg L^{-1}, $pH_0 = 3.0$, $C_{0(Fe)} = 7.5$ g L^{-1}, $C_{0(GAC)} = 12.5$ g L^{-1}, and $[H_2O_2]_0 = 22.8$ mmol L^{-1}

Fenton system for 7-h reaction. However, the defluorination ratio of PFOA ascended to 46.81 % when adding a certain amount of H_2O_2 (22.8 mmol L^{-1}). It indicated that the dosage of appropriate H_2O_2 had a positive influence on removal of PFOA.

H_2O_2 was the original source of generating OH· radicals; hence, increasing H_2O_2 dosage was favorable to promoting decomposition of PFOA. Nevertheless, it was the possibility that iron hydroxide precipitation was formed between ferric and OH^- at higher H_2O_2 concentration, resulting in the decreasing of photocatalytic degradation PFOA when H_2O_2 was added excessively (22.8 mmol L^{-1}). Therefore, excess H_2O_2 dosage was unfavorable for PFOA defluorination. Furthermore, the competition of photons may occur between lots of hydroxyl radical (OH·) and PFOA, resulting in the reduction of PFOA absorption photons and degradation efficiency of PFOA by direct photolysis (185-nm VUV). At this time, the efficient impact of OH· could not make up for the negative effect of the photon competition on the defluorination of PFOA. Hence, the optimized H_2O_2 dosage was 22.8 mmol L^{-1} in the experiment.

Valence state and content of iron in Fe^0/GAC micro-electrolysis and VUV-Fenton system

Valence state and content of iron was major component in the system which could affect defluorination of PFOA in photocatalytic degradation. Hence, the concentrations of irons with different valence states were monitored using 1,10-phenanthroline spectrophotometric method ($\lambda_{max} - 510$ nm) in this section (Fig. 6). The results found that the concentrations of Fe^{2+} and total iron rapidly decreased with the reaction time in Fe^0/GAC micro-electrolysis and VUV-Fenton system. However, the concentration of Fe^{3+} had diverse variation.
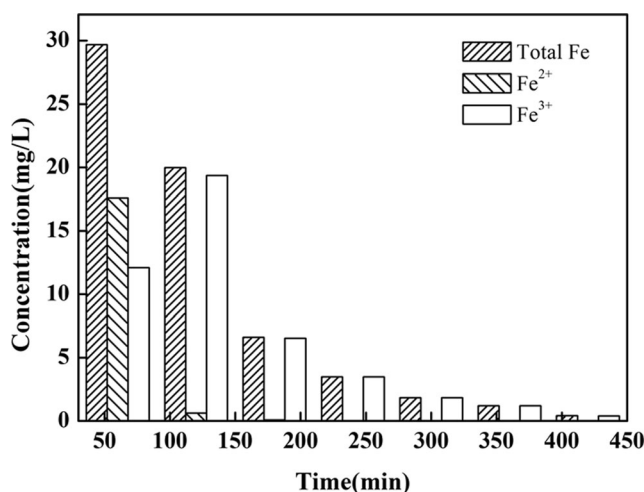
Firstly, the concentration of Fe^{3+} increased up to 19.37 mg L^{-1} within 2 h but quickly decreased as the extension of reaction time.

The experiment was conducted under the atmosphere, which Fe^{2+} was gradually oxidized to Fe^{3+}. Because of the existence of OH^- in the system, plenty of ferric hydroxide was generated with the passage of time, leading to the reducing of the Fe concentration.

Analysis of intermediate products in the system

As shown in the "Effects of VUV photolysis system on photodegradation of PFOA" section, the defluorination efficiency was inconsistent with PFOA degaradation ratio, and the degradation ratio much more than defluorination efficiency, meaning that PFOA was not completely mineralized to CO_2 and F^-. Thus, besides fluoride ion, the intermediates of shorter-chain perfluorocarboxylic acid ($C_nF_{2n+1}COO^-$, PFCAs), including PFHpA (C7), PFHeA (C6), PFPeA (C5), PFBA (C4), PFPrA (C3), and TPA (C2), were monitored by HPLC/MS/MS analysis with retention time of 5.65, 5.25, 4.58, 2.72, 1.32, and 1.28 min, respectively, suggesting the formation of PFCA ions in Fe^0/GAC micro-electrolysis and VUV-Fenton system. The perfluoroalkyl compounds with longer carbon chains generally have higher peak concentrations than those with shorter chains. The decomposition intermediates were the same as those reported by other researchers (Cheng et al. 2014; Tang et al. 2012; Wang et al. 2010; Cao et al. 2010; Wang et al. 2008; Wang and Zhang 2014; Zoschke et al. 2014). Figure 7 shows the total ion chromatography (TIC) of seven kinds of PFCA standard samples. External standard method was used for measurement of PFCAs.

The degradation of PFOA and intermediates were shown in Fig. 8a. The formation of the five kinds of PFCAs, including
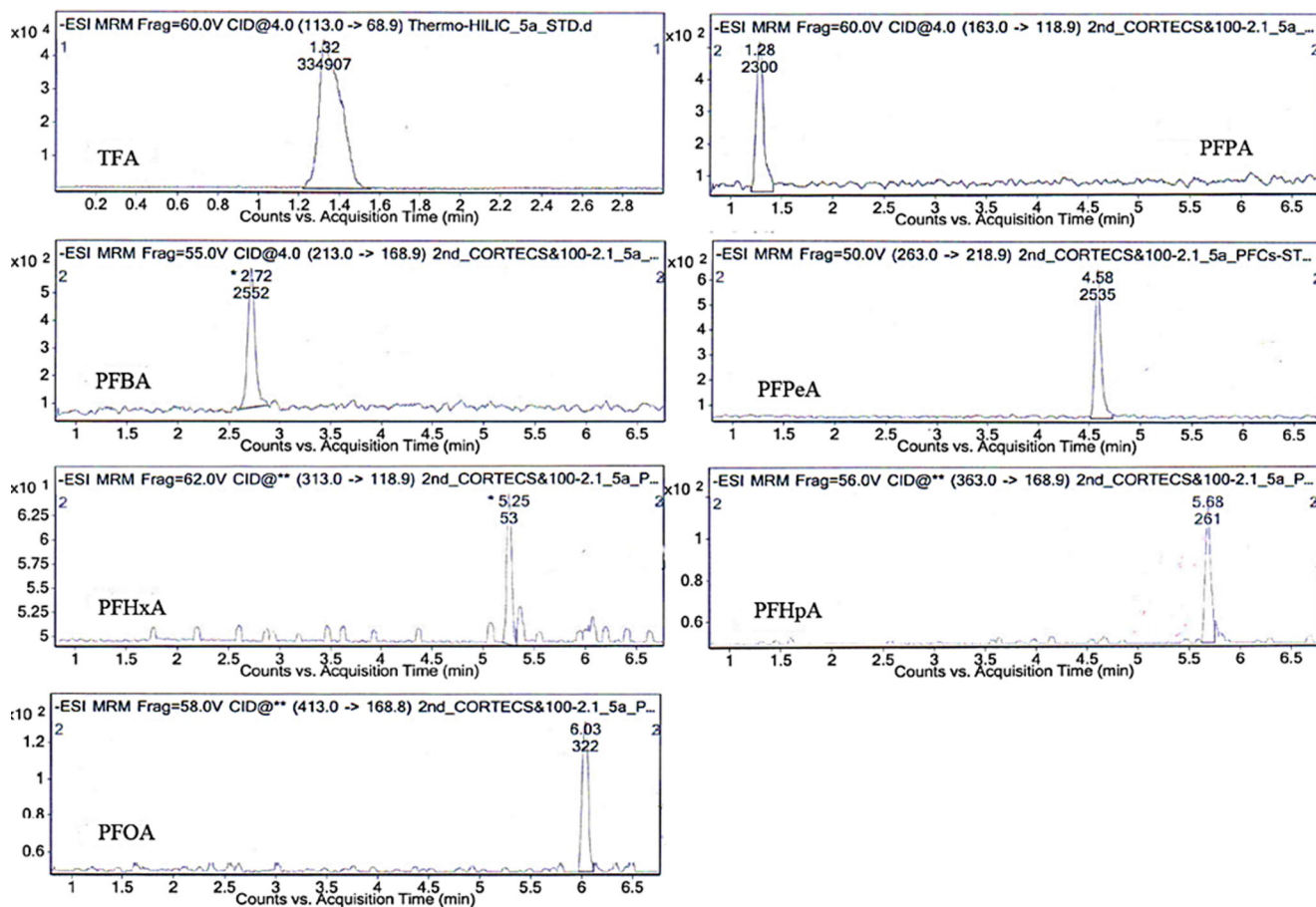
Fig. 7 MRM spectra of standard solution of seven kinds of PFCAs

PFHpA (with one CF_2 unit less than PFOA), PFHeA (with two CF_2 units less than PFOA), PFPeA (with three CF_2 units less than PFOA), PFBA (with four CF_2 units less than PFOA),

and PFPrA (with five CF_2 units less than PFOA), increased continuously in the degradation process after 5 h. Especially, PFHpA had obviously changed. Nevertheless, TPA was not
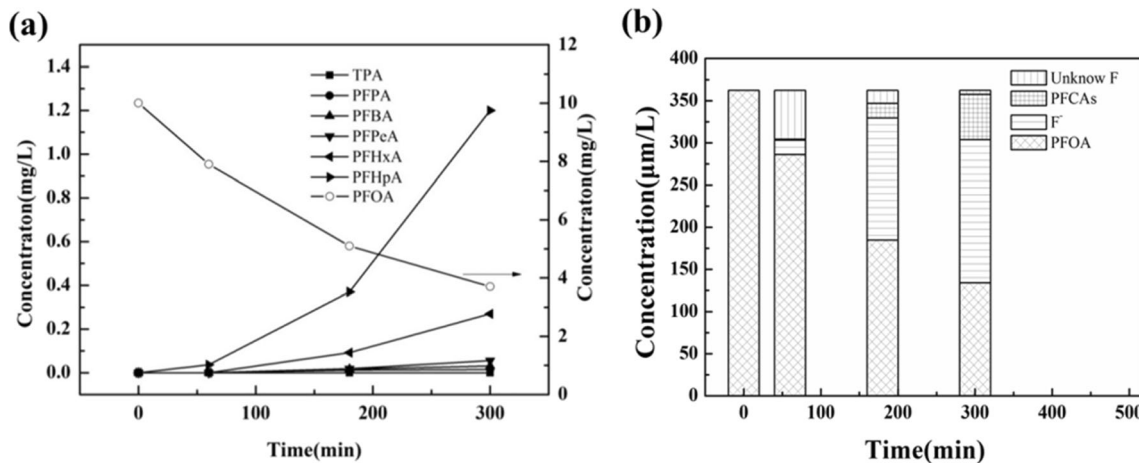

Fig. 8 **a** Evolution of the decomposition of PFOA and the intermediates in system. **b** Fluorine element mass balance during the decomposition of PFOA. $C_{0(PFOA)} = 10$ mg L^{-1}, $pH_0 = 3.0$, $C_{0(Fe)} = 7.5$ g L^{-1}, $C_{0(GAC)} = 12.5$ g L^{-1}, and $[H_2O_2]_0 = 22.8$ mmol L^{-1}

detected in the whole reaction process. In addition, PFHpA was firstly monitored after 1 h of reaction (Fe^0/GAC micro-electrolysis process), indicating that PFOA could be decomposed by Fe^0/GAC micro-electrolysis process. Moreover, the shorter-chain intermediates were identified after about 2 h of reaction, indicating that PFCAs may be formed and degraded stepwise.

In order to further study the decomposition of PFOA process in Fe^0/GAC micro-electrolysis and VUV-Fenton system, the mass balance of fluorine element (F^-) was also calculated for the reaction system (Fig. 8b). The total F content in aqueous solution consists of the following three sections: organic fluorine, F^-, and unknown fluoride. The mass concentration of the organic fluorine in the solutions was analyzed using fluoride ion selective electrode (PF-1-01) after the different reaction time. The organic fluorine mainly referred to the fluorine in PFOA and intermediates which were detected by HPLC/MS/MS, and their mass concentrations were calculated from mass ration between fluorine and parent PFCAs.

$$Y = \sum_{i=0}^{6} (3 + 2i) \times C_{CF_3(CF_2)_i COO^-} \qquad (7)$$

The unknown fluorine was those not to be identified by above analysis. The unknown F mass concentration was calculated by subtracting both the kinds of fluorine mentioned above from total fluorine. The results of analysis of mass balance of fluorine were given in Fig. 8b. Aqueous organic fluorine and inorganic fluorine accounted for more than 85 % of the fluorine in the decomposed PFOA solution at any point during the reaction process. In Fig. 8b, it was found that the amounts of organic fluorine lost and inorganic fluoride ion formed in the solution were very similar, indicating that the lost organic fluorine might be converted into fluorine ions during degradation. Due to the very low proportion of unknown fluorine, it could be inferred that shorter-chain PFCs were main intermediate products of PFOA during reaction in Fe^0/GAC micro-electrolysis and VUV-Fenton system.
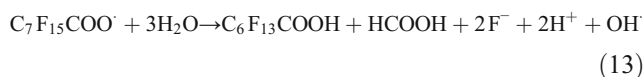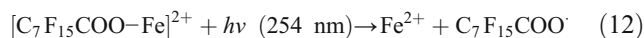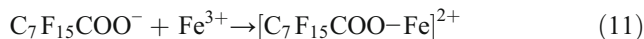
Defluorination and decomposition mechanisms of PFOA

As reported in literature (Tang et al. 2012), PFOA was degraded by the attack of OH· radicals with UV light irradiation. Tang et al. investigated that PFOA was stimulated by OH· radicals and changed PFOA*, then decarboxylated into C_7F_{15}· and CO_2 by breaking the C-C bond between the C_7F_{15} and $COO-$. Furthermore, the C_7F_{15}· radical was immediately hydrolyzed and converted into the $C_6F_{13}COOH$ and fluoride ion. The intermediate $C_6F_{13}COOH$ was further

decomposed into a series of perfluorinated carboxylic acids in a similar pathway.

$$C_7F_{15}COO^- + OH \cdot \rightarrow C_7F_{15}COO \cdot + OH^- \qquad (8)$$

$$C_7F_{15}COO \cdot \rightarrow CO_2 + C_7F_{15} \cdot \qquad (9)$$

$$C_7F_{15} \cdot + 2H_2O \rightarrow C_6F_{13}COOH + 2F^- + 2H^+ + H \qquad (10)$$

It were also reported that (Cheng et al. 2014; Wang et al. 2008; Hori et al. 2007) ferric ions could form a complex with PFOA, and then, the complex could be converted to Fe^{2+} and organic radical under the UV 254-nm light irradiation. Hori et al. (2007) investigated that the complex was formed between Fe^{3+} and C_2F_5COOH at first and was then stimulated and photolysis by 220–460-nm UV light irradiation. Moreover, they indicated that Fe^{3+} could be transformed into Fe^{2+} after reaction under oxygen atmosphere during the photochemical degradation of C_2F_5COOH. They also found that the $[C_2F_5COO-Fe]^{2+}$ was a prerequisite species for the photochemical degradation of C_2F_5COOH under 220–460-nm UV light irradiation on the basis of electron spin resonance (ESR) spectrum of the mixture of iron (III) sulfate and C_2F_5COOH.

$$C_7F_{15}COO^- + Fe^{3+} \rightarrow [C_7F_{15}COO-Fe]^{2+} \qquad (11)$$

$$[C_7F_{15}COO-Fe]^{2+} + h\nu \ (254 \ nm) \rightarrow Fe^{2+} + C_7F_{15}COO \cdot \qquad (12)$$

$$C_7F_{15}COO \cdot + 3H_2O \rightarrow C_6F_{13}COOH + HCOOH + 2F^- + 2H^+ + OH^- \qquad (13)$$

$$Fe^{2+} + O_2 \rightarrow Fe^{3+} + O_2 \cdot^- \qquad (14)$$

$$Fe^{2+} + OH \cdot \rightarrow Fe^{3+} + OH^- \qquad (15)$$

Cheng et al. (2014) investigated that PFOA could be excited by VUV 185-nm light irradiation converted to C_7F_{15}· and COOH·. Then, C_7F_{15}· was hydrolyzed to $C_7F_{15}OH$ in water, and $C_7F_{15}OH$ further formed $C_7F_{13}COF$ and fluoride ion by losing a CF_2 unit. Finally, the $C_7F_{13}COF$ was transformed into $C_7F_{13}COOH$ in water. The $C_7F_{13}COOH$ was decomposed to shorter-chain PFCAs by a similar pathway. And, fluoride ion was continuously generated from CF_2 unit removed from PFCAs.

$$C_8F_{15}COOH + h\nu \ (185 \ nm) \rightarrow C_7F_{15} \cdot + COOH \cdot \qquad (16)$$

$$C_7F_{15} \cdot + H_2O \rightarrow C_7F_{15}OH + H \qquad (17)$$

$$C_7F_{15}OH \rightarrow C_7F_{13}COF + H^+ + F^- \qquad (18)$$

$$C_7F_{13}COF + H_2O \rightarrow C_6F_{13}COOH + H^+ + F^- \qquad (19)$$
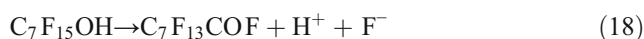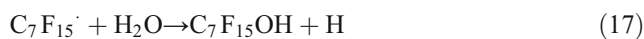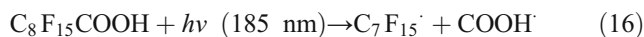
As mentioned above, during removal of PFOA, fluoride ion was also continuously formed. Furthermore, five shorter-chain PFCs, including C7, C6, C5, C4, and C3, were detected by HPLC/MS/MS during decomposition of PFOA, and their concentrations also continuously increased and had the following sequence during reaction time: C7 > C6 > C5 > C4 > C3. These showed that degradation of PFOA was a stepwise way. Firstly, PFOA was transformed into $C_6F_{13}COOH$ with a less CF_2 unit than PFOA, and then $C_6F_{13}COOH$ into $C_5F_{11}COOH$, $C_5F_{11}COOH$ into C_4F_9COOH, and C_4F_9COOH into C_3F_7COOH, through a similar pathway. The CF_2 unit removed from the PFCAs was transformed to formic acid (or further mineralized as CO_2) and fluoride ion.

Based on the discussions above and the experimental results, the mechanisms of degradation and defluorination of PFOA with Fe^0/GAC and VUV-Fenton system were proposed. Photochemical of OH·, direct photolysis, and photocatalysis were involved in the reaction solution (Fig. 9). Photochemical of OH·, with OH· radicals and UV, PFOA was stimulated by OH· radicals and changed PFOA*, then the C-C bond between the C_7F_{15} and COO− was broke into C_7F_{15}· and CO_2. Next, the C_7F_{15}· radical was

immediately hydrolyzed and converted into the $C_6F_{13}COOH$ and fluoride ion. The intermediate $C_6F_{13}COOH$ further was decomposed into a series of perfluorinated carboxylic acids in a similar pathway. Direct photolysis (185 nm), with VUV 185-nm irradiation, the C-C bond in the PFOA between C_7F_{15} and COO− was fractured and produced C_7F_{15}· radical. Then, the C_7F_{15}· radical was hydrolyzed in water and generated the $C_7F_{15}OH$. And, the $C_7F_{15}OH$ further transformed into acyl fluoride and $C_6F_{13}COF$ by losing a HF unit. Ultimately, the $C_6F_{13}COF$ was produced to a shorter-chain $C_6F_{13}COOH$ in water. Photocatalytic degradation of PFOA in the presence of Fe^{3+} (UV 254 nm), the complex was formed between PFOA and Fe^{3+}, and then, the complex was excited and photolyzed by UV 254-nm light irradiation for formation of the $C_7F_{15}COO$·. The $C_7F_{15}COO$· radical could generate $C_6F_{13}COOH$ with less CF_2 unit than the PFOA in water, and fluoride ions were formed. The intermediate $C_6F_{13}COOH$ was able to further be decomposed to shorter-chain PFCAs in a similar pathway.

As the above analysis, PFOA could be degraded and defluorinated to shorter-chain PFCAs through photochemical of OH·, direct photolysis (VUV 185-nm light), and
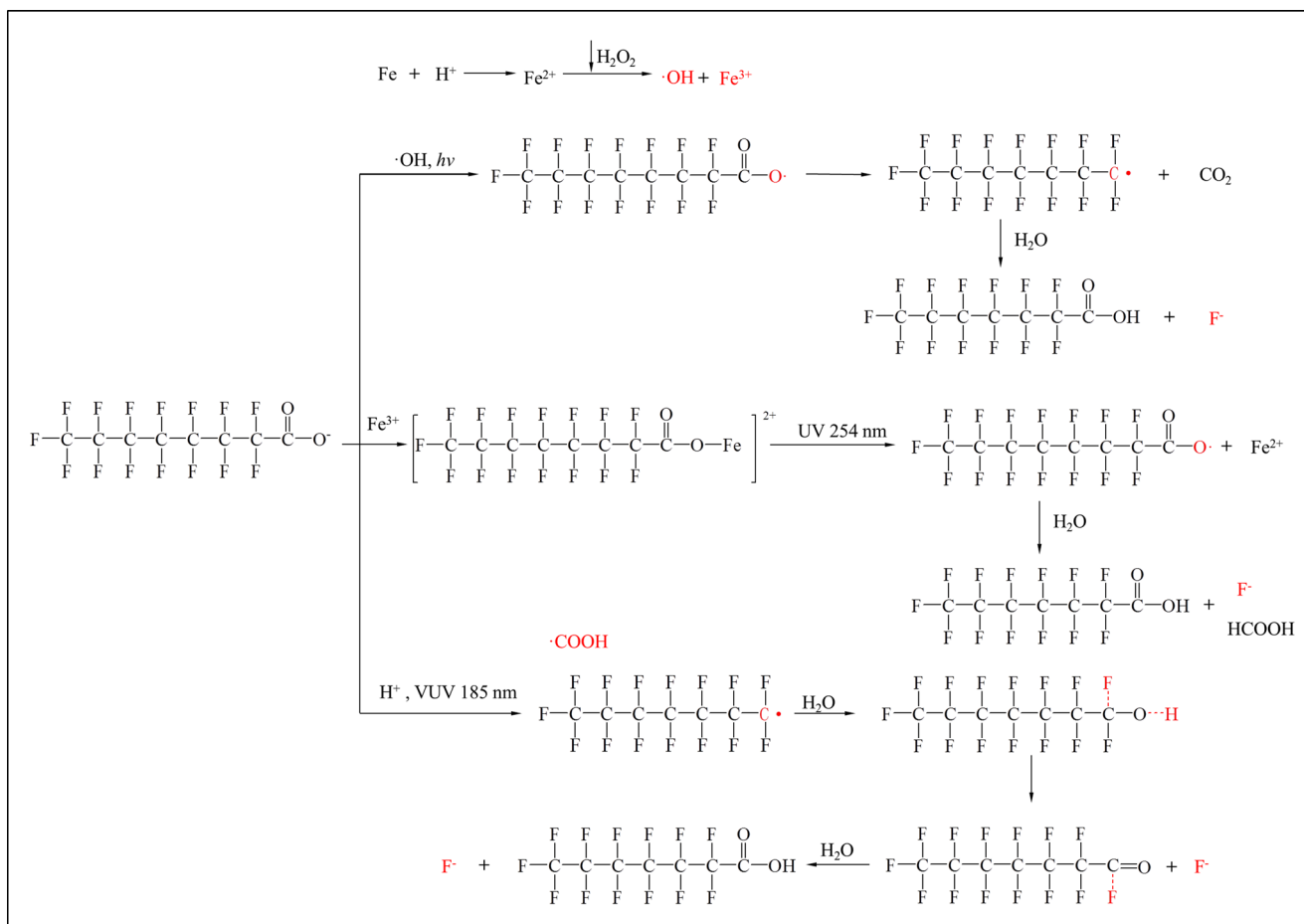

Fig. 9 Possible defluorination and decomposition pathways of PFOA in Fe^0/GAC micro-electrolysis and VUV-Fenton system

photocatalytic degradation in a stepwise way. The CF_2 unit that came from PFCAs was transformed to CO_2 and fluoride ion. If the reaction time was long enough, PFOA and the intermediates could be completely mineralized to CO_2 and fluoride ion.

Conclusions

The Fe^0/GAC micro-electrolysis and VUV-Fenton system were employed for the defluorination of PFOA. Under the conditions of initial experiment, pH 3.0, Fe^0 dosage 7.5 g L^{-1}, GAC dosage 12.5 g L^{-1}, and H_2O_2 concentration 22.8 mmol L^{-1}, the defluorination of PFOA reached 46.81 %. Furthermore, the intermediates of degradation PFOA were short-chain PFCAs, including PFHpA (C7), PFHeA (C6), PFPeA (C5), PFBA (C4), PFPrA (C3), and TPA (C2), which were identified and quantified using HPLC/MS/MS. According to the mass balance calculation, the decomposition of PFOA and intermediates always was step-by-step through loss of a CF_2. It is proposed that photochemical of OH·, direct photolysis, and photocatalysis are referred to the reaction solution.

References

Abbott BD, Wood CR, Watkins AM, Tatum-Gibbs K, Das KP, Lau C (2012) Effects of perfluorooctanoic acid (PFOA) on expression of peroxisome proliferator-activated receptors (PPAR) and nuclear receptor-regulated genes in fetal and postnatal CD-1 mouse tissues. Reprod Toxicol 33:491–505

Amonette JE, Templeton JC (1998) Improvements to quantitative the assay of nonrefractory minerals for Fe (II) and total Fe using 1,10-phenanthroline. Clay Clay Miner 46:51–62

Blake DK, Robert DH, Craig SC (1997) Fluorinated organics in the biosphere. Environ Sci Technol 31:2445–2454

Butenhoff JL, Chang SC, Olsen GW, Thomford PJ (2012) Chronic dietary toxicity and carcinogenicity study with ammonium perfluorooctanoate in Sprague-Dawley rats. Toxicology 298:1–13

Cao MH, Wang BB, Yu HS, Wang LL, Yuan SH, Chen J (2010) Photochemical decomposition of perfluorooctanoic acid in aqueous periodate with VUV and UV light irradiation. J Hazard Mater 179:1143–1146

Chen J, Zhang PY, Liu J (2007) Photodegradation of perfluorooctanoic acid by 185 nm vacuum ultraviolet light. J Environ Sci-China 19:387–390

Cheng JH, Liang XY, Yang SW, Hu YY (2014) Photochemical defluorination of aqueous perfluorooctanoic acid (PFOA) by VUV/Fe^{3+} system. Chem Eng J 239:242–249

Dai JY, Li M, Jin YH, Saito N, Xu MQ, Wei FW (2006) Perfluorooctanesulfonate and perfluorooctanoate in red panda and giant panda from China. Environ Sci Technol 40:5647–5652

Ding G, Zhang J, Chen Y, Wang L, Wang M, Xiong D, Sun Y (2013) Combined effects of PFOS and PFOA on zebrafish (*Danio rerio*) embryos. Arch Environ Con Tox 64:668–675

Dinglasan-Panlilio MJ, Prakash SS, Baker JE (2014) Perfluorinated compounds in the surface waters of Puget Sound, Washington and Clayoquot and Barkley Sounds, British Columbia. Mar Pollut Bull 78:173–180

Fan L, Ni J, Wu Y, Zhang Y (2009) Treatment of bromoamine acid wastewater using combined process of micro-electrolysis and biological aerobic filter. J Hazard Mater 162:1204–1210

Florentin A, Deblonde T, Diguio N, Hautemaniere A, Hartemann P (2011) Impacts of two perfluorinated compounds (PFOS and PFOA) on human hepatoma cells: cytotoxicity but no genotoxicity? Int J Hyg Envir Heal 214:493–499

Geiger SD, Xiao J, Ducatman A, Frisbee S, Innes K, Shankar A (2014) The association between PFOA, PFOS and serum lipid levels in adolescents. Chemosphere 98:78–83

Gisey JP, Kannan K (2001) Global distribution of perfluorooctane sulfonate in wildlife. Environ Sci Technol 35:1339–1342

Guan X, Xu X, Lu M, Li H (2012) Pretreatment of oil shale retort wastewater by acidification and ferric-carbon micro-electrolysis. In: International Conference on Future Electrical Power and Energy System. Energy Procedia 1655-1661

Heydebreck F, Tang JH, Xie ZY, Ebinghaus R (2015) Alternative and legacy perfluoroalkyl substances: differences between European and Chinese river/estuary systems. Environ Sci Technol 49:8386–8395

Hori H, Yamamoto A, Koike K, Kutsuna S, Osaka I, Arakawa R (2007) Photochemical decomposition of environmentally persistent short-chain perfluorocarboxylic acids in water mediated by iron(II)/(III) redox reactions. Chemosphere 68:572–578

Houde M, Letcher JW, Martin RJ, Solomon KR, Muir DCG (2006) Biological monitoring of polyfluoroalkyl substances: a review. Environ Sci Technol 40:3462–3473

Hu Q, Franklin JN, Bryan I, Morris E, Wood A, DeWitt JC (2012) Does developmental exposure to perfluorooctanoic acid (PFOA) induce immunopathologies commonly observed in neurodevelopmental disorders? Neurotoxicology 33:1491–1498

Huang L, Sun G, Yang T, Zhang B, He Y, Wang X (2013a) A preliminary study of anaerobic treatment coupled with micro-electrolysis for anthraquinone dye wastewater. Desalination 309:91–96

Huang LH, Sun GP, Yang T, Zhang B, He Y, Wang XH (2013b) A preliminary study of anaerobic treatment coupled with micro-electrolysis for anthraquinone dye wastewater. Desalination 309:91–96

Johansson N, Eriksson P, Viberg H (2009) Neonatal exposure to PFOS and PFOA in mice results in changes in proteins which are important for neuronal growth and synaptogenesis in the developing brain. Toxicol Sci 108:412–418

Lai B, Zhou Y, Yang P, Yang J, Wang J (2013) Degradation of 3,3′-iminobis-propanenitrile in aqueous solution by Fe(0)/GAC micro-electrolysis system. Chemosphere 90:1470–1477

Lau C, Anitole K, Hodes C, Lai D, Pfahles-Hutchens A, Seed J (2007) Perfluoroalkyl acids: a review of monitoring and toxicological findings. Toxicol Sci 99:366–394

Lee YC, Lo SL, Chiueh PT, Liou YH, Chen ML (2010) Microwave-hydrothermal decomposition of perfluorooctanoic acid in water by iron-activated persulfate oxidation. Water Res 44:886–892

Li G, Guo S, Li F (2010) Treatment of oilfield produced water by anaerobic process coupled with micro-electrolysis. J Environ Sci-China 22:1875–1882

Liu WW, Tu XY, Wang XP, Wang FQ, Li W (2012) Pretreatment of coking wastewater by acid out, micro-electrolysis process with in situ electrochemical peroxidation reaction. Chem Eng J 200–202:720–728

Loos R, Locoro G, Huber T, Wollgast J, Christoph EH, De Jager A, Gawlik BM, Hanke G, Umlauf G, Zaldivar JM (2008) Analysis of

perfluorooctanoate (PFOA) and other perfluorinated compounds (PFCs) in the River Po watershed in N-Italy. Chemosphere 71: 306–313

Loos R, Gawlik BM, Locoro G, Rimaviciute E, Contini S, Bidoglio G (2009) EU-wide survey of polar organic persistent pollutants in European river waters. Environ Pollut 157:561–568

Lv Y, Wang Y, Shan M, Shen X, Su Y (2011) Denitrification of coking wastewater with micro-electrolysis. J Environ Sci-China 23:S128–S131

Poothong S, Boontanon SK, Boontanon N (2012) Determination of perfluorooctane sulfonate and perfluorooctanoic acid in food packaging using liquid chromatography coupled with tandem mass spectrometry. J Hazard Mater 205–206:139–143

Qin L, Zhang G, Meng Q, Xu L, Lv B (2012) Enhanced MBR by internal micro-electrolysis for degradation of anthraquinone dye wastewater. Chem Eng J 210:575–584

Shoeib M, Harner T, Vlahos P (2006) Perfluorinated chemicals in the Arctic atmosphere. Environ Sci Technol 40:7577–7583

Tang H, Xiang Q, Lei M, Yan J, Zhu L, Zou J (2012) Efficient degradation of perfluorooctanoic acid by UV–Fenton process. Chem Eng J 184:156–162

Vaalgamaa S, Vahatalo AV, Perkola N, Huhtala S (2011) Photochemical reactivity of perfluorooctanoic acid (PFOA) in conditions representing surface water. Sci Total Environ 409:3043–3048

Wang Y, Zhang P (2014) Effects of pH on photochemical decomposition of perfluorooctanoic acid in different atmospheres by 185 nm vacuum ultraviolet. J Environ Sci-China 26:2207–2214

Wang Y, Zhang P, Pan G, Chen H (2008) Ferric ion mediated photochemical decomposition of perfluorooctanoic acid (PFOA) by 254 nm UV light. J Hazard Mater 160:181–186

Wang BB, Cao MH, Tan ZJ, Wang LL, Yuan SH, Chen J (2010) Photochemical decomposition of perfluorodecanoic acid in aqueous solution with VUV light irradiation. J Hazard Mater 181:187–192

Wang X, Gong X, Zhang Q, Du H (2013) Degradation mechanism of Direct Pink 12B treated by iron-carbon micro-electrolysis and Fenton reaction. J Environ Sci-China 25:S63–S68

Wania F (2007) A global mass balance analysis of the source of perfluorocarboxylic acids in the Arctic ocean. Environ Sci Technol 41:4529–4535

Yang SW, Sun J, Hu YY, Cheng JH, Liang XY (2013) Effect of vacuum ultraviolet on ultrasonic defluorination of aqueous perfluorooctanesulfonate. Chem Eng J 234:106–114

Yen Le TT, Peijnenburg WJGM (2013) Modeling toxicity of mixtures of perfluorooctanoic acid and triazoles (triadimefon and paclobutrazol) to the benthic cladoceran Chydorus sphaericus. Environ Sci Technol 47:6621–6629

Yeung LWY, Robinson SJ, Koschorreck J, Mabury SA (2013) Part I. A temporal study of PFCAs and their precursors in human plasma from two German cities 1982–2009. Environ Sci Technol 47: 3864–3874

Ying D, Xu X, Li K, Wan YG, Jia J (2012) Design of a novel sequencing batch internal micro-electrolysis reactor for treating mature landfill leachate. Chem Eng Res Des 90:2278–2286

Zhang C, Zhou M, Ren G, Yu X, Ma L, Yang J, Yu F (2015) Heterogeneous electro-Fenton using modified iron-carbon as catalyst for 2,4-dichlorophenol degradation: influence factors, mechanism and degradation pathway. Water Res 70:414–424

Zhou H, Lv P, Shen Y, Wang J, Fan J (2013) Identification of degradation products of ionic liquids in an ultrasound assisted zero-valent iron activated carbon micro-electrolysis system and their degradation mechanism. Water Res 47:3514–3522

Zhu Q, Guo S, Guo C, Dai D, Jiao X, Ma T, Chen J (2014) Stability of Fe-C micro-electrolysis and biological process in treating ultra-high concentration organic wastewater. Chem Eng J 255:535–540

Zoschke K, Bornick H, Worch E (2014) Vacuum-UV radiation at 185 nm in water treatment—a review. Water Res 52:131–145